Journal of Gastroenterology and Hepatology

Dynamic computed tomography is useful for prediction of pathological grade in pancreatic neuroendocrine neoplasm

Journal:	*Journal of Gastroenterology and Hepatology*
Manuscript ID	JGH-00662-2016.R1
Manuscript Type:	Original Article - Biliary and Pancreatic
Date Submitted by the Author:	n/a
Complete List of Authors:	Horiguchi, Shigeru; Okayama University Graduate School of Medicine, Dentistry, and Pharmaceutical Sciences, Gastroenterology and Hepatology Kato, Hironari; Okayama University Graduate School of Medicine, Dentistry, and Pharmaceutical Sciences, Gastroenterology and Hepatology Shiraha, Hidenori; Okayama University Graduate School of Medicine, Dentistry, and Pharmaceutical Sciences , Gastroenterology and Hepatology Tsutsumi, Koichiro; Okayama University Graduate School of Medicine, Dentistry, and Pharmaceutical Science, Gastroenterology and Hepatology Yamamoto, Naoki; Okayama University Graduate School of Medicine, Dentistry, and Pharmaceutical Science, Gastroenterology and Hepatology Matsumoto, Kazuyuki; Okayama University Graduate School of Medicine, Dentistry and Pharmaceutical Science, Gastroenterology and Hepatology Tomoda, Takeshi; Okayama University Graduate School of Medicine, Dentistry, and Pharmaceutical Sciences, Gastroenterology & Hepatology Uchida, Daisuke; Okayama University Graduate School of Medicine, Dentistry, and Pharmaceutical Science, Gastroenterology and Hepatology Akimoto, Yutaka; Okayama University Graduate School of Medicine, Dentistry, and Pharmaceutical Sciences, Department of Gastroenterology & Hepatology Mizukawa, Syou; Okayama University Graduate School of Medicine, Dentistry, and Pharmaceutical Sciences, Gastroenterology and Hepatology Tanaka, Takehiro; Okayama University Graduate School of Medicine, Dentistry and Pharmaceutical Sciences, Pathology and Oncology Ichimura, Koichi; Okayama University Graduate School of Medicine, Dentistry, and Pharmaceutical Sciences, Department of Pathology Takaki, Akinobu; Okayama University Graduate School of Medicine, Dentistry, and Pharmaceutical Sciences , Gastroenterology and Hepatology Yagi, Takahito; Okayama University Graduate School of Medicine, Dentistry and Pharmaceutical Sciences, Department of Gastroenterological Surgery Okada, Hiroyuki; Okayama University Graduate School of Medicine, Dentistry, and Pharmaceutical Sciences, Department of Gastroenterology and Hepatology
Key Words:	pancreatic neuroendocrine neoplasm, pathological grade, WHO2010, dynamic CT, MVD

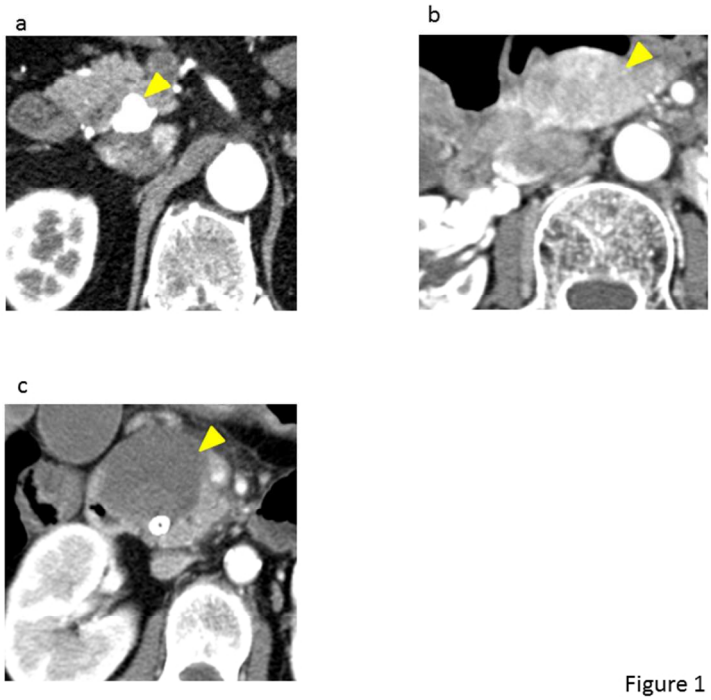

Figure 1

Figure 1
CT images of PNEN with pathological grade, G1, G2 and G3 at artery phase of dynamic CT. Pathological grade 1 (1A) is very high density, and grade 3 (1C) is very low. Grade 2 (1B) is intermediate between grade 1 and 3. Each arrow indicates the tumor.

254x190mm (96 x 96 DPI)

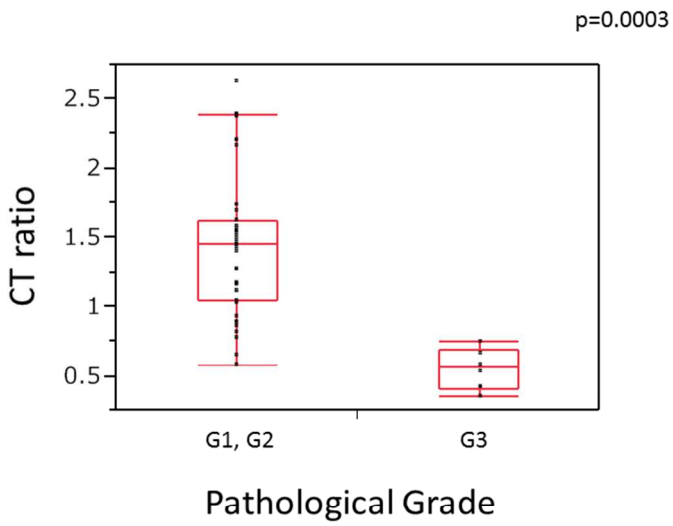

Figure 2

Figure 2
The relationship between pathological grade (G1+G2, G3) and CT ratio. Between G1+G2 and G3, CT ratio has significant difference (p=0.0003).

254x190mm (96 x 96 DPI)

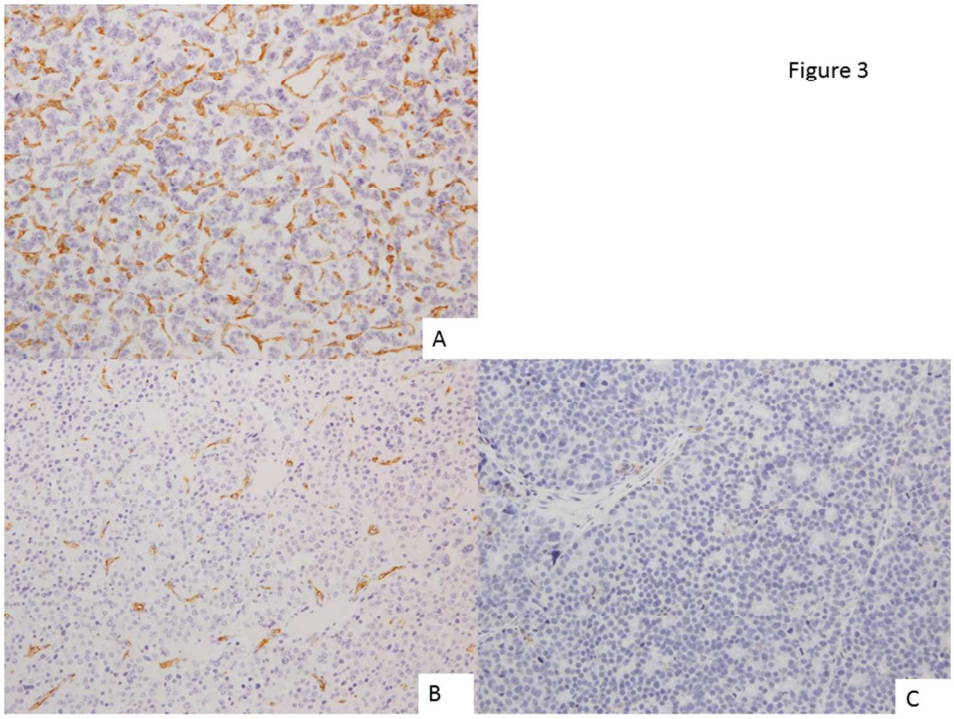

Figure 3
Three examples of CD31 immunostaining of PNEN are shown. Brownish area is CD31 positive area.

Figure 3A
Immunohistochemical staining of CD31 in G1 PNEN. Intratumoral microvascular density (MVD) is high, and the microvessel is long.

Figure 3B
Immunohistochemical staining of CD31 in G2 PNEN. The MVD of G2 is lower than that of G1, and the length of microvessel is shorter than that of G1.

Figure 3C
Immunohistochemical staining of CD31 in G3 PNEN. MVD is very low and almost all microvessels are not seen in G3.

254x190mm (96 x 96 DPI)

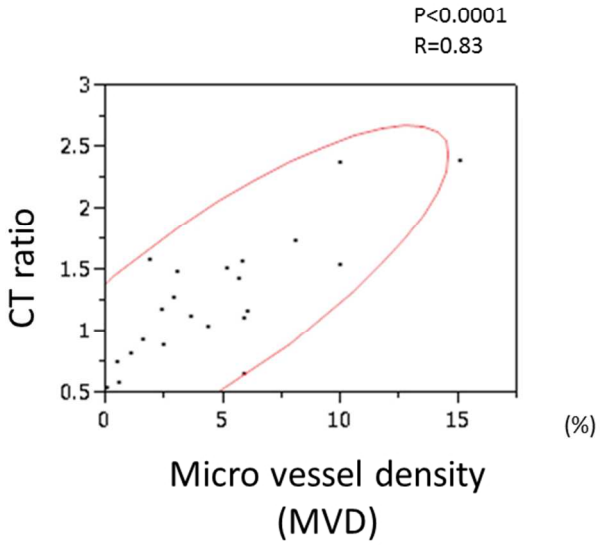

Figure 4

Figure 4
MVD has a significant correlation with CT ratio in arterial phase (r=0.83, p<0.0001)

254x190mm (96 x 96 DPI)

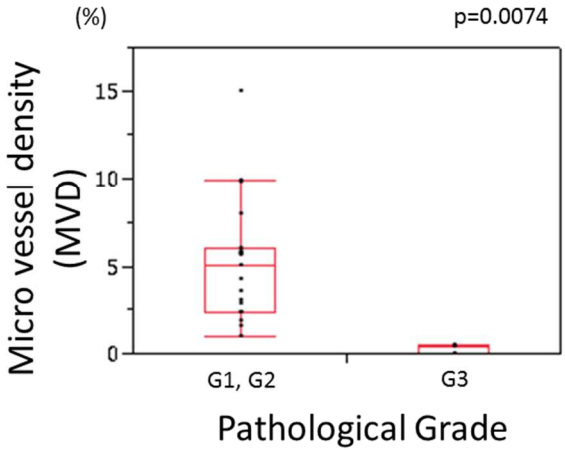

Figure 5

Figure 5
MVD has a significant correlation with pathological grade (p=0.0074)

254x190mm (96 x 96 DPI)

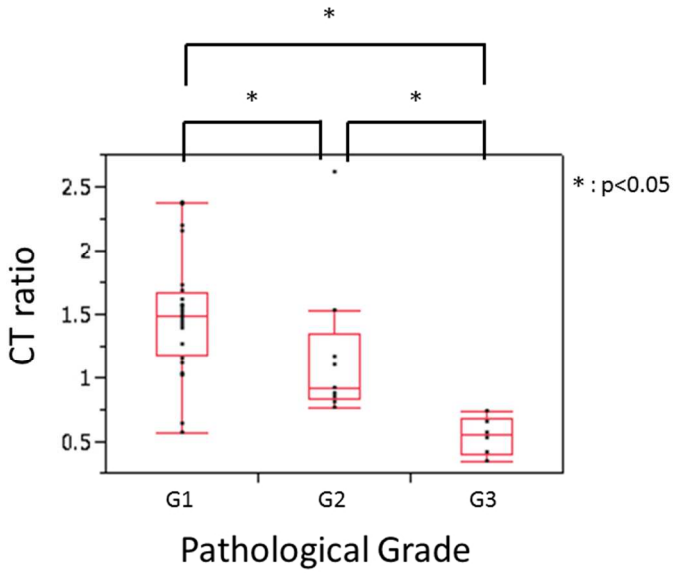

Supplemental figure1

Supplemental figure 1
The relationship between pathological grade (G1, G2, G3) and CT ratio. Between G1 and G2; G2 and G3; and G3 and G1, CT ratio has significant difference ($p<0.05$).

254x190mm (96 x 96 DPI)

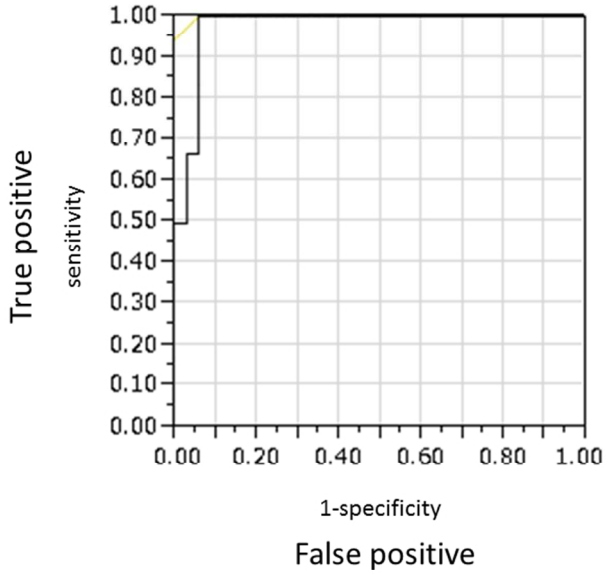

Supplemental figure 2

Supplemental figure 2
Receiver operating characteristic (ROC) curve for prediction of G3 with CT ratio. The area under the receiver operating characteristic curve (AUROC) is 0.97. The cut-off value of CT ratio between the G1, G2, and G3 determined by the ROC analysis was 0.75.

254x190mm (96 x 96 DPI)

Table 1 Clinical and histological characteristics of patients

	All cases (n = 39)
Male/Female	15/24
Age (mean ± SD)	55 ± 14
MEN1/VHL	3/2
Position	
Head /Body/Tail	20/12/7
Tumor diameter (mm) (mean ± SD)	29 ± 25
Tumor type	
Functional/Non-functional	6/33
Hormonal type	
Insulinoma	3
Gastrinoma	2
Glucagonoma	1
Pathological classification	
G1/G2/G3	24/9/6
TNM classification	
I/II/III/IV	16/11/3/9

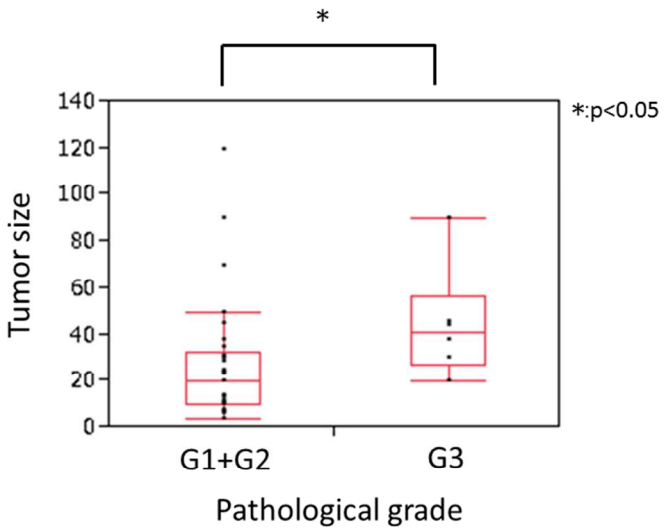

Supplemental figure 4

Supplemental Figure 4
The relationship between pathological grade (G1+G2, G3) and tumor size. The G3 tumors are larger than tumors of G1 and G2 ($p < 0.05$).

254x190mm (96 x 96 DPI)

Dynamic computed tomography is useful for prediction of pathological grade in pancreatic neuroendocrine neoplasm

Shigeru Horiguchi[1], Hironari Kato[1], Hidenori Shiraha[1], Koichiro Tsutsumi[1], Naoki Yamamoto[1], Kazuyuki Matsumoto[1], Takeshi Tomoda[1], Daisuke Uchida[1], Yutaka Akimoto[1], Syou Mizukawa[1], Takehiro Tanaka[2], Koichi Ichimura[2], Akinobu Takaki[1], Takahito Yagi[3], Hiroyuki Okada[1]

[1] Department of Gastroenterology and Hepatology in Okayama University Graduate School of Medicine, Dentistry, and Pharmaceutical Science, Okayama, Japan

[2] Department of Pathology and Oncology in Okayama University Graduate School of Medicine, Dentistry and Pharmaceutical Sciences, Okayama, Japan

[3] Department of Gastroenterological Surgery in Okayama University Graduate School of Medicine, Dentistry and Pharmaceutical Sciences, Okayama, Japan

Correspondence

Shigeru Horiguchi, Department of Gastroenterology and Hepatology in Okayama Medical University, 2-5-1 Shikata-cho, Kita-ku, Okayama city, Japan 700-8551

E-mail: horiguchis@gmail.com

Tel +81-86-235-7221

Fax +81-86-225-5991

Disclosure statement

We have no conflicts of interest to declare.

Acknowledgements

We would like to thank Taiko Kameyama for her expert technical assistance.

Abstract

Background and Aim: Pathological grading is important in defining the therapeutic strategy in pancreatic neuroendocrine neoplasm (PNEN), but is difficult for unresectable cases. Endoscopic ultrasound (EUS)-guided fine needle aspiration (FNA) is useful in the diagnosis of PNEN, but its usefulness for pathological grading is not well established. No studies have examined the diagnostic ability of dynamic computed tomography (CT) for pathological grading of PNEN. We investigated the usefulness of EUS-FNA and dynamic CT in the diagnosis and pathological grading of PNEN.

Methods: In this retrospective study, 39 PNEN patients finally diagnosed via EUS-FNA and/or surgical resection underwent dynamic CT. Pathological samples were diagnosed based on WHO2010; staging was based on the ENETS classification. The proportion of the quantification value in the tumor to the pancreatic parenchyma in arterial phase was defined as the CT ratio. Immunohistochemical staining with CD31 was performed to evaluate microvessel density (MVD). We evaluated the relationship between pathological grade, CT ratio, and MVD.

Results: By using EUS-FNA, 35 of 39 (90%) cases were diagnosed as PNEN. As for pathological grade, 15 of 35 (43%) cases could be identified correctly. CT ratio could predict pathological grade 3 disease. The sensitivity, specificity, and diagnostic accuracy were 100%, 94%, and 95%. MVD was significantly correlated with CT ratio ($r = 0.83$, p

< 0.0001) and pathological grade (p = 0.0074).

Conclusions: CT ratio has a relationship with pathological grade in PNEN, which would help decide therapeutic strategy in unresectable cases and cases in which pathological grading is difficult.

Key words: dynamic CT, microvessel density, pancreatic neuroendocrine neoplasm, pathological grade, WHO2010

Introduction

Pancreatic neuroendocrine neoplasms (PNENs) are rare tumors derived from the hormone-producing cells in the pancreas islet of Langerhans and precursors in the ductal epithelium.[1] The crude annual incidence per 100,000 is 5.3 in the United States[1,2] and 2.2 in Japan.[3] PNEN is commonly regarded as a low- to intermediate-grade neuroendocrine neoplasm.[4] However, in some patients, especially those with distant metastasis, the condition progressively worsens. Yao et al. reported that the median survival time in regional stage and distant stage was 77 months and 24 months, respectively, from SEER registry data.[4,5]

The World Health Organization (WHO) defined the pathological classification of PNEN in the WHO2010 grading system, in which PNEN is classified into Grade 1 (G1), Grade 2 (G2), and Grade 3 (G3) according to the mitotic activity and Ki-67 labeling index.[6] This classification is commonly used and is useful for the prognosis of PNEN.[2,7,8] The WHO2010 grading system is also very useful for determining a therapeutic strategy.

Although the prognosis after curative resection for patients with PNEN is relatively fair, the prognosis for unresectable patients is poor.[5] For the patients with unresectable PNEN, therapeutic options are transcatheter arterial chemoembolization (TACE), radiofrequency ablation (RFA), somatostatin analogue, sunitinib, streptozocin, oral inhibitor of mammalian target of rapamycin (mTOR), and peptide receptor-targeted radiotherapy (PRRT).[9] These are particularly applicable in the unresectable G1 and G2 cases.[9–11] However, in cases of unresectable neuroendocrine carcinoma (NEC), combination chemotherapy using platinum plus etoposide is recommended as per NCCN and ESMO guidelines.[9,12] In Japan, combination chemotherapy using platinum

plus irinotecan is also used.[13] However, no satisfactory survival rates have been achieved in these cases yet.[9,13] In this way, there is significant difference between G1, G2, and G3 cases on therapeutic strategy and survival duration. Therefore, the identification of pathological grade is very important for unresectable case to be treated appropriately.

Hasegawa et al. reported the usefulness of endoscopic ultrasound (EUS)-guided fine needle aspiration (FNA) for the diagnosis of PNEN[14]; however, the usefulness of EUS-FNA for pathological grading is still not well established.[15,16] The operation sample or enough volume of biopsy sample are needed for accurate pathological grading. However, it is sometimes difficult to obtain a sufficient sample for unresectable cases. Other modalities for prediction of pathological grade may be helpful to decide the therapeutic strategy.

Many reports stated that the majority of PNENs are enhanced clearly following intravenous injection of contrast medium. In particular, tumor-to-pancreas contrast is usually greatest in arterial phase.[17–20] Inversely, it is reported that characteristic finding of small cell cancer of pancreas takes on a slight enhanced effect with CT using contrast agent.[21] However, there is no detailed report about the correlation between pathological grade based on WHO2010 and quantitative evaluation of the enhancement on enhanced CT.

Angiogenesis is essential for tumor growth, invasion, and metastasis, and Marion-Audibert et al. reported the correlation between angiogenesis and survival with PNEN.[22] Measurement of the microvessel density (MVD) has been reported as a reliable marker for tumor angiogenesis. Therefore, evaluation of tumor angiogenesis by measuring the

MVD may be an important prognostic factor. However, the relationship between MVD and pathological grade or between MVD and enhancement on dynamic CT is unclear.

We performed a retrospective study of a series of PNENs in order to determine whether quantitative evaluation of the enhancement on dynamic CT predicts the WHO2010 pathological grade. Additionally, we investigated the relationship between enhancement on enhanced CT, pathological grade, and quantitative evaluation of intratumoral MVD.

To our knowledge, this is the first report to show a correlation between quantitative evaluation of enhancement on dynamic CT and pathological grade based on WHO2010 and MVD.

Methods

Patients. In this retrospective study, we enrolled 39 patients who were diagnosed with PNEN by using histopathological or cytological analysis of samples obtained via EUS-FNA and/or operation samples at the Okayama University Hospital from December 2007 to March 2012. All 39 patients underwent dynamic CT and EUS-FNA. Surgery was performed for all G1 and G2 patients and for 2 of 6 (33%) G3 patients. These pathological samples were carefully examined by two pathologists (T.T and K.I) based on the WHO2010 classification. The tumor staging of all patients was performed using CT according to the European Neuroendocrine Tumor Society (ENETS) guidelines.

CT protocol. Triphasic spiral CT was performed using MDCT (Aquilion; TOSHIBA, Tokyo, Japan). The scanning parameters were 120 kVp, 150 mAs, 2-mm section

collimation and an 11.0 mm/s table speed, during a single-breath-hold helical acquisition period of 20–25 s. Images were obtained in a craniocaudal direction and were reconstructed every 5 mm to obtain contiguous sections. The bolus tracking method was used for scanning in each patient. With a power injector, 2 mL/kg of nonionic iodinated contrast agent (iopamidol, Iopamiron 370; Shering, Berlin, Germany) was injected in the antecubital vein at a flow rate of 4.0 mL/s. The arterial phase, portal venous phase, and delayed phase spiral scans were automatically started 12, 32, and 180 s, respectively, after exceeding the contrast enhancement threshold level in the lumen of the descending aorta.

Quantitative evaluation of dynamic CT. To evaluate the enhancement of tumor, we defined CT ratio as the ratio of CT value of the tumor to that of normal pancreatic parenchyma in the arterial phase. CT values were quantified by using Hounsfield unit thresholds by placing a region of interest (ROI) at three points. The ratio of each mean CT ratio of tumor to that of parenchyma was calculated. CT values were measured by one of the authors (N.Y), who was blinded to the clinical information. ROIs at the tumor were placed on the lowest density area with taking care to avoid the pancreatic duct and cystic lesion.

EUS-FNA and pathological evaluation. We used a convex echoendoscope (UCT260; Olympus Optical Co. Ltd., Tokyo, Japan) connected to a US device (α10; Aloka, Tokyo, Japan). After detecting the objective tumor, we performed fine needle aspiration by using a 19-gauge, 22-gauge, or 25-gauge needle (EchoTip-Ultra needle; Cook Medical, Limerick, Ireland). The selection of diameter of needle depended on the tumor size and

the blood flow volume of the tumor. A part of the aspirated materials was immediately evaluated by using Diff Quick staining by a cytopathologist for rapid onsite evaluation (ROSE). After ROSE, the remaining material was fixed in 10% formalin in a specimen bottle. The specimens that were too small to assess as materials for histopathological diagnosis were centrifuged, and then embedded in paraffin for cell-block analysis. Sections were subjected to hematoxylin and eosin staining and immunohistochemical staining and were then evaluated by two independent pathologists (T.T and K.I).

Hematoxylin and eosin staining and immunohistochemistry. The formalin-fixed specimens were processed into paraffin according to standard routine methods, and 5-μm sections were stained with hematoxylin and eosin for conventional histology and were assessed as detailed in the WHO2010 guidelines. Immunohistochemistry was performed according to standard routine methods. We used the primary antibodies against CD31 (M0823; Dako Japan), chromogranin A (clone LK2H10), synaptophysin (clone SP11) (Automated Slide Preparation System BenchMark XT; Ventana Medical Systems Inc., Tucson, Ariz) and Ki-67 (clone MIB-1; Dako, Glostrup, Denmark). Primary antibodies were detected using secondary antibody (Dako Japan), and the signal was developed with diaminobenzidine, followed by hematoxylin counterstaining.

Evaluation of MVD. To determine MVD, the tissue sections stained with CD31 were screened under low magnification (×40) and the most vascularized areas within tumors were selected; the three selected areas were photographed using a digital camera under high magnification (×100) (BX51 and DP50; Olympus, Tokyo, Japan). The recorded images had a resolution of 1 920,000 pixels. CD31 immunohistochemistry was

performed in all surgical samples of G1 and G2 cases and two resectable G3 cases. In the four unresectable G3 cases, CD31 immunohistochemistry was performed in EUS-FNA samples. To calculate the MVD, the areas occupied by CD31-positive microvascular was quantified using Adobe Photoshop (version CS6; Adobe Systems). The average MVDs of the three selected areas were calculated as percentages of the CD31-stained area in a field of tumor sections. The sections were independently scored by two observers (Y.N and K.T) blinded to the clinical data of the patients.

Statistical analysis. Statistical analysis was performed using JMP8 (SAS, USA). Chi-square test or Student's t- test were used to analyze variables. A probability of $p < 0.05$ was considered statistically significant.

Results

Patients. Table 1 shows the clinical and histological characteristics of the patients. In our data, all G3 cases and 4 of 9 G2 (44%) cases had distant metastasis. Prediction of pathological grade depending on the presence of distant metastasis was not easy. All G1 cases and 5 of 9 (56%) G2 cases underwent definitive operation. The remaining four G2 patients with distant metastasis underwent debulking or bypass operation. Of six patients with G3, one underwent curative pancreaticoduodenectomy and another patient underwent only bypass operation because of peritoneal dissemination; the other four patients received chemotherapy after pathological diagnosis with EUS-FNA.

Diagnostic ability of EUS-FNA. Thirty-five of 39 (90%) cases could be diagnosed with PNEN with EUS-FNA. Three of four cases could not be diagnosed correctly

because of lack of sufficient specimen. One case was misdiagnosed as sarcoma. The diagnosis rate for neuroendocrine neoplasm was 92%, 78%, and 100% for G1, G2, and G3 cases, respectively. Of the 35 cases diagnosed with PNEN by using EUS-FNA, pathological grade could be identified in only 15 (43%) cases. The pathological grade identification rate of EUS-FNA was 45%, 0%, and 83% for G1, G2, and G3 cases, respectively.

Diagnostic ability of dynamic CT. Figure 1 shows that representative CT images of pathological grade 1, 2, and 3 at the artery phase. An expert radiologist checked the dynamic CT findings. Eighteen of 19 (95%) patients of typical hypervascular tumors were diagnosed correctly. Three of 13 (23%) hypovascular cases were misdiagnosed as pancreatic ductal carcinoma. Two of seven (29%) patients with slightly hypervascular cases were misdiagnosed with intraductal papillary mucinous carcinoma (IPMCa) or gastrointestinal stromal tumor (GIST). PNEN was aggressively suspected in 26 of 39 (67%) cases based on clinical imaging findings on dynamic CT. Twenty of 26 (77%) cases were graded as G1, 5 (19%) as G2, and 1 of 6 (4%) as G3.

Diagnostic ability of dynamic CT for CT ratio. ROIs were placed on the lowest density area while taking care to avoid the pancreatic duct and cystic lesion. In this study, we could not find necrotic tissue in any of the 39 patients. The CT ratio had significant correlation with each pathological grade (Supplemental Figure 1). The ratios in the G3 cases were significantly lower than those in the G1 and G2 cases ($p = 0.0003$) (Figure 2). The area under the receiver operating characteristic curve (AUROC) for prediction of G3 with CT ratio was 0.97 (Supplemental Figure 2). The sensitivity,

specificity, positive predictive value (PPV), negative predictive value (NPV), and diagnosis accuracy were 100%, 94%, 75%, 100%, and 95%, respectively with the cut-off value of CT ratio, 0.75, by the ROC analysis.

Correlation between MVD and CT value ratio. Three examples of CD31 immunostaining of PNEN are shown in Figure 3. The brownish area is the CD31-positive area (magnification: ×100). Figure 3A shows G1 PNEN. Intratumoral MVD is high, and the length of microvessels is long. Figure 3B shows G2 PNEN. The MVD of G2 is lower than that of G1, and the length of microvessels is shorter than that of G1. Figure 3C shows G3 PNEN. MVD is very low and almost no microvessel can be seen in G3. MVD has a significant correlation with CT ratio ($r = 0.83$, $p < 0.0001$) (Figure 4) and pathological grade ($p = 0.0074$) (Figure 5).

Discussion

The prognosis of PNEN differs depending on pathological grade and is unfavorable in patients with G3 disease.[2,4,5,7,8,11] Some effective therapies are reported in unresectable G1 and G2 cases,[9–11] but in G3 cases, which are almost always unresectable, the prognosis is unsatisfactory.[9] Therefore, pathological grading is a very important factor for deciding the therapeutic strategy, and in the surgical resection cases, it is easy to obtain enough samples for pathological grading.

In our study, 4 of 9 (44%) G2 cases (three, liver metastasis; one, liver and bone metastasis) and 5 of 6 (83%) G3 cases had distant metastasis of the liver (Table 1). Therefore, the presence or absence of distant metastasis does not always have a

relationship with pathological grade. It is also very important to diagnose pathological grade in unresectable cases because of distant metastasis or other reasons.

The usefulness of EUS-FNA for the diagnosis of PNEN has been reported in many papers, and its accuracy has been estimated at 83–93%.[23–26] In our study, 35 of 39 (90%) cases were diagnosed as PNEN. We also verified whether the EUS-FNA is useful for prediction of pathological grade per the WHO2010. Ten of 29 (34%) G1 and G2 cases and 5 of 6 (83%) G3 cases were accurately predicted using EUS-FNA. Except for five unresectable cases that were diagnosed as grade 3 with EUS-FNA samples because of the high Ki67 index, EUS-FNA samples were checked against the surgical samples. There was one case, which, at first, was determined as G1 via EUS-FNA, but was finally determined to be G3 after assessing the surgical sample. In this case, inadequate specimen with EUS-FNA misled the pathological grading. Previous studies have described the strong ability of EUS-FNA to predict pathological grade,[15,27–29] but there was no proof of surgical sample or exact validation between FNA and surgical samples,[15,27,28] or there was a discrepancy in the Ki67 labeling between the cytological and surgical samples, except for high Ki67 labeling.[29] In cases of a discrepancy in Ki67 labeling between EUS-FNA and surgical samples, pathological evaluation using EUS-FNA samples may not provide accurate findings. Hasegawa et al. stated that concordance rates of pathological grade between EUS–FNA samples and resected specimens are 74.0% when using the mean Ki-67 index in EUS–FNA specimens and 77.8% when using the highest Ki-67 index. [14] In addition, the concordance rate rises to 90% when EUS–FNA samples with less than 2000 tumor cells are excluded. However, it is often difficult for an unskilled endoscopist to obtain more than 2000 tumor cells. In addition, it is also difficult to obtain information on the number of cells

from on-site examination, and repeated needling for obtaining enough tumor cells may sometimes result in complications such as bleeding. These results suggest that diagnosis of PNEN is possible by using EUS-FNA, but pathological grading is often difficult. In our study, the diagnosis rate of pathological grade was low (43% for all pathological grades). Therefore, the diagnosis rate using EUS-FNA samples might depend on the technical level, which may lead to variation between facilities.

PNEN shows varied enhancement on dynamic CT.[17–21,30] As shown in Figure 1A, tumors with typical findings are easy to diagnose, but some neoplasms cannot be differentiated from pancreatic adenocarcinomas.[31] Therefore, the diagnostic accuracy of dynamic CT is insufficient, with 64–81% of sensitivity.[32] In our study, only 67% of patients could be initially diagnosed with suspected PNEN on dynamic CT alone. All tumors diagnosable by CT are hypervascular (Figure 1A), whereas hypovascular tumors (Figure 1B, 1C) are difficult to diagnose. This shows that dynamic CT alone is not always useful for diagnosis of PNEN.

We found a correlation between WHO2010 pathological grade and enhanced effect on dynamic CT. There was an evident negative correlation between CT ratio and pathological grade ($p < 0.05$) (Supplemental Figure 1), in particular G3 (Figure 2). Some reports have shown that tumor-to-pancreas contrast is usually greatest in the arterial phase in PNEN cases.[17,18,20,31] Therefore, we used arterial phase images to evaluate the enhancement and calculate the CT ratio. By using ROC curve analysis to understand the association between CT ratio and pathological grade, the cut-off value of CT ratio value was calculated. Based on this cut-off value of 0.75, pathological G3 could be accurately identified with significant probability. We believe that CT ratio is extremely useful for prediction of pathological grade. CT ratio does not rely on

technical skills, which would reduce the differences across facilities. CT ratio was also significantly correlated with tumor size. CT ratio was higher in smaller tumors ($p = 0.016$) (Supplementary Figure 3). Moreover, tumor size was significantly correlated with pathological grade. In G3 patients, tumor size (median size: 41 mm) was larger than in G1 and G2 patients (median size: 20 mm) ($p = 0.029$) (Supplementary Figure 4). However, tumor size is not useful for predicting the pathological grade. The sensitivity, specificity, PPV, NPV, and diagnosis accuracy were 83%, 67%, 31%, 96%, and 69%, respectively, with a cut-off value of tumor size of 30 mm by the ROC analysis (Supplementary Figure 5).

By using pathological samples, we found that the decrease in the CT ratio was significantly correlated with decreased MVD (Figure 4). The correlation between enhanced effect in dynamic CT and MVD has been reported in lung cancer,[33] hepatic cellular carcinoma,[34] pancreatic ductal adenocarcinoma,[35] prostate disease,[36] and mammary adenocarcinoma.[37,38] Moreover, one study showed that MVD decrease is a predictive factor of prognosis, and MVD has significant negative correlation with Ki67 index in PNEN.[22] In that study, Marion-Audibert et al. showed that well-differentiated neuroendocrine neoplasms can induce the maintenance of organoid features in their microenvironment, including a high microvascular density recalling the situation in the normal pancreatic neuroendocrine tissue. Thus, the MVD has a significant relationship with the Ki67 index, and it is a very important factor in the clinical course of this disease. Our research shows MVD had a correlation with CT ratio (Figure 4) and pathological grade (Figure 5). These results indicate that MVD is high in G1, low in G3, and intermediate in G2, and CT ratio can reflect the MVD in each pathological grade. Therefore, we believe that CT ratio in dynamic CT is useful for predicting the

pathological grade.

In conclusion, CT ratio in dynamic CT is related to pathological grade in PNEN. Moreover, we identified a relationship between CD31 expression in the tumor and pathological grade. CT ratio is thought to reflect MVD, and prediction of pathological grade with dynamic CT ratio is possible. After diagnosis of PNEN with EUS-FNA, CT ratio with dynamic CT is very useful for predicting the pathological grade of PNEN. In this way CT ratio is very useful to decide the therapeutic strategy, in particular for unresectable cases in which adequate sample is difficult to obtain for pathological grading. To our knowledge, this is the first report that states that there is a correlation between quantitative evaluation of enhancement on dynamic CT, pathological grade based on WHO2010, and MVD.

Acknowledgements

We would like to thank Taiko Kameyama for her expert technical assistance.

References

1 Asa SL. Pancreatic endocrine tumors. Mod Pathol 2011; 24 Suppl 2: S66–77.

2 Kulke MH, Benson AB, 3rd, Bergsland E, Berlin JD, Blaszkowsky LS, Choti MA, et al. Neuroendocrine tumors. J Natl Compr Canc Netw 2012; 10: 724–64.

3 Ito T, Sasano H, Tanaka M, Osamura RY, Sasaki I, Kimura W, et al. Epidemiological study of gastroenteropancreatic neuroendocrine tumors in Japan. J. Gastroenterol 2010; 45: 234–43.

4 Yao JC, Eisner MP, Leary C, Dagohoy C, Phan A, Rashid A, et al. Population-based study of islet cell carcinoma. Ann Surg Oncol 2007; 14: 3492–500.

5 Yao JC, Hassan M, Phan A, Dagohoy C, Leary C, Mares JE, et al. One hundred years after "carcinoid": epidemiology of and prognostic factors for neuroendocrine tumors in 35,825 cases in the United States. J Clin Oncol 2008; 26: 3063–72.

6 Kloppel G. Classification and pathology of gastroenteropancreatic neuroendocrine neoplasms. Endocr. Relat. Cancer 2011; 18 Suppl 1: S1–16.

7 Pape UF, Jann H, Muller-Nordhorn J, Bockelbrink A, Berndt U, Willich SN, et al. Prognostic relevance of a novel TNM classification system for upper gastroenteropancreatic neuroendocrine tumors. Cancer 2008; 113: 256–65.

8 Hochwald SN, Zee S, Conlon KC, Colleoni R, Louie O, Brennan MF, et al. Prognostic factors in pancreatic endocrine neoplasms: an analysis of 136 cases with a proposal for low-grade and intermediate-grade groups. J Clin Oncol 2002; 20: 2633–42.

9 Oberg K, Knigge U, Kwekkeboom D, Perren A, Group EGW. Neuroendocrine gastro-entero-pancreatic tumors: ESMO Clinical Practice Guidelines for diagnosis, treatment and follow-up. Ann Oncol 2012; 23 Suppl 7: vii124–30.

10 Oberg KE, Reubi JC, Kwekkeboom DJ, Krenning EP. Role of somatostatins in

gastroenteropancreatic neuroendocrine tumor development and therapy. Gastroenterology 2010; 139: 742–53, 53 e1.

11 Yao JC, Shah MH, Ito T, Bohas CL, Wolin EM, Van Cutsem E, et al. Everolimus for advanced pancreatic neuroendocrine tumors. N Engl J Med 2011; 364: 514–23.

12 Kulke MH, Shah MH, Benson AB, 3rd, Bergsland E, Berlin JD, Blaszkowsky LS, et al. Neuroendocrine tumors, version 1.2015. J Natl Compr Canc Netw 2015; 13: 78–108.

13 Yamaguchi T, Machida N, Morizane C, Kasuga A, Takahashi H, Sudo K, et al. Multicenter retrospective analysis of systemic chemotherapy for advanced neuroendocrine carcinoma of the digestive system. Cancer Sci 2014; 105: 1176–81.

14 Hasegawa T, Yamao K, Hijioka S, Bhatia V, Mizuno N, Hara K, et al. Evaluation of Ki-67 index in EUS-FNA specimens for the assessment of malignancy risk in pancreatic neuroendocrine tumors. Endoscopy 2014; 46: 32–8.

15 Alexiev BA, Darwin PE, Goloubeva O, Ioffe OB. Proliferative rate in endoscopic ultrasound fine-needle aspiration of pancreatic endocrine tumors: correlation with clinical behavior. Cancer 2009; 117: 40–5.

16 Yang Z, Tang LH, Klimstra DS. Effect of tumor heterogeneity on the assessment of Ki67 labeling index in well-differentiated neuroendocrine tumors metastatic to the liver: implications for prognostic stratification. Am J Surg Pathol 2011; 35: 853–60.

17 Rockall AG, Reznek RH. Imaging of neuroendocrine tumours (CT/MR/US). Best Pract Res Clin Endocrinol Metab 2007; 21: 43–68.

18 Van Hoe L, Gryspeerdt S, Marchal G, Baert AL, Mertens L. Helical CT for the

preoperative localization of islet cell tumors of the pancreas: value of arterial and parenchymal phase images. AJR Am J Roentgenol 1995; 165: 1437–9.

19 Chung MJ, Choi BI, Han JK, Chung JW, Han MC, Bae SH. Functioning islet cell tumor of the pancreas. Localization with dynamic spiral CT. Acta Radiol 1997; 38: 135–8.

20 Stafford-Johnson DB, Francis IR, Eckhauser FE, Knol JA, Chang AE. Dual-phase helical CT of nonfunctioning islet cell tumors. J Comput Assist Tomogr 1998; 22: 335–9.

21 Ichikawa T, Federle MP, Ohba S, Ohtomo K, Sugiyama A, Fujimoto H, et al. Atypical exocrine and endocrine pancreatic tumors (anaplastic, small cell, and giant cell types): CT and pathologic features in 14 patients. Abdom Imaging 2000; 25: 409–19.

22 Marion-Audibert AM, Barel C, Gouysse G, Dumortier J, Pilleul F, Pourreyron C, et al. Low microvessel density is an unfavorable histoprognostic factor in pancreatic endocrine tumors. Gastroenterology 2003; 125: 1094–104.

23 Ardengh JC, de Paulo GA, Ferrari AP. EUS-guided FNA in the diagnosis of pancreatic neuroendocrine tumors before surgery. Gastrointest Endosc 2004; 60: 378–84.

24 Larghi A, Verna EC, Ricci R, Seerden TC, Galasso D, Carnuccio A, et al. EUS-guided fine-needle tissue acquisition by using a 19-gauge needle in a selected patient population: a prospective study. Gastrointest Endosc 2011; 74: 504–10.

25 Gornals J, Varas M, Catala I, Maisterra S, Pons C, Bargalló D, et al. Definitive diagnosis of neuroendocrine tumors using fine-needle aspiration-puncture guided by endoscopic ultrasonography. Rev Esp Enferm Dig 2011; 103: 123–8.

26 Gines A, Vazquez-Sequeiros E, Soria MT, Clain JE, Wiersema MJ. Usefulness

of EUS-guided fine needle aspiration (EUS-FNA) in the diagnosis of functioning neuroendocrine tumors. Gastrointest Endosc 2002; 56: 291–6.

27 Chatzipantelis P, Konstantinou P, Kaklamanos M, Apostolou G, Salla C. The role of cytomorphology and proliferative activity in predicting biologic behavior of pancreatic neuroendocrine tumors: a study by endoscopic ultrasound-guided fine-needle aspiration cytology. Cancer 2009; 117: 211–6.

28 Larghi A, Capurso G, Carnuccio A, Ricci R, Alfieri S, Galasso D, et al. Ki-67 grading of nonfunctioning pancreatic neuroendocrine tumors on histologic samples obtained by EUS-guided fine-needle tissue acquisition: a prospective study. Gastrointest Endosc 2012; 76: 570–7.

29 Piani C, Franchi GM, Cappelletti C, Scavini M, Albarello L, Zerbi A, et al. Cytological Ki-67 in pancreatic endocrine tumours: an opportunity for pre-operative grading. Endocr Relat Cancer 2008; 15: 175–81.

30 Rha SE, Jung SE, Lee KH, Ku YM, Byun JY, Lee JM. CT and MR imaging findings of endocrine tumor of the pancreas according to WHO classification. Eur J Radiol 2007; 62: 371–7.

31 Gritzmann N, Macheiner P, Hollerweger A, Hubner E. CT in the differentiation of pancreatic neoplasms--progress report. Dig. Dis. 2004; 22: 6–17.

32 Vick C, Zech CJ, Hopfner S, Waggershauser T, Reiser M. [Imaging of neuroendocrine tumors of the pancreas]. Der Radiologe 2003; 43: 293–300.

33 Yi CA, Lee KS, Kim EA, Han J, Kim H, Kwon OJ, et al. Solitary pulmonary nodules: dynamic enhanced multi-detector row CT study and comparison with vascular endothelial growth factor and microvessel density. Radiology 2004; 233: 191–9.

34 Matsubara M, Shiraha H, Kataoka J, Iwamuro M, Horiguchi S, Nishina S, et al.

Des-gamma-carboxyl prothrombin is associated with tumor angiogenesis in hepatocellular carcinoma. J Gastroenterol Hepatol 2012; 27: 1602–8.

35 Wang ZQ, Li JS, Lu GM, Zhang XH, Chen ZQ, Meng K. Correlation of CT enhancement, tumor angiogenesis and pathologic grading of pancreatic carcinoma. World J Gastroenterol 2003; 9: 2100–4.

36 Wilson NM, Masoud AM, Barsoum HB, Refaat MM, Moustafa MI, Kamal TA. Correlation of power Doppler with microvessel density in assessing prostate needle biopsy. Clin Radiol 2004; 59: 946–50.

37 Buadu LD, Murakami J, Murayama S, Hashiguchi N, Sakai S, Masuda K, et al. Breast lesions: correlation of contrast medium enhancement patterns on MR images with histopathologic findings and tumor angiogenesis. Radiology 1996; 200: 639–49.

38 Frouge C, Guinebretiere JM, Contesso G, Di Paola R, Blery M. Correlation between contrast enhancement in dynamic magnetic resonance imaging of the breast and tumor angiogenesis. Invest Radiol 1994; 29: 1043–9.

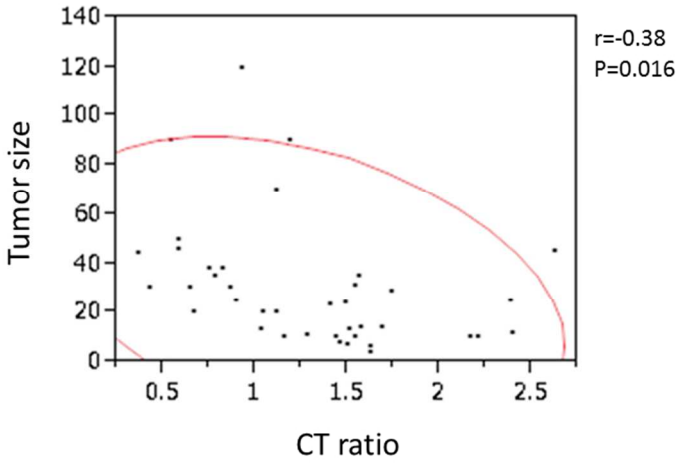

Supplemental figure 3

Supplemental Figure 3
The relationship between CT ratio and tumor size. CT ratio is higher in smaller tumors (p = 0.016, r = -0.38).

254x190mm (96 x 96 DPI)

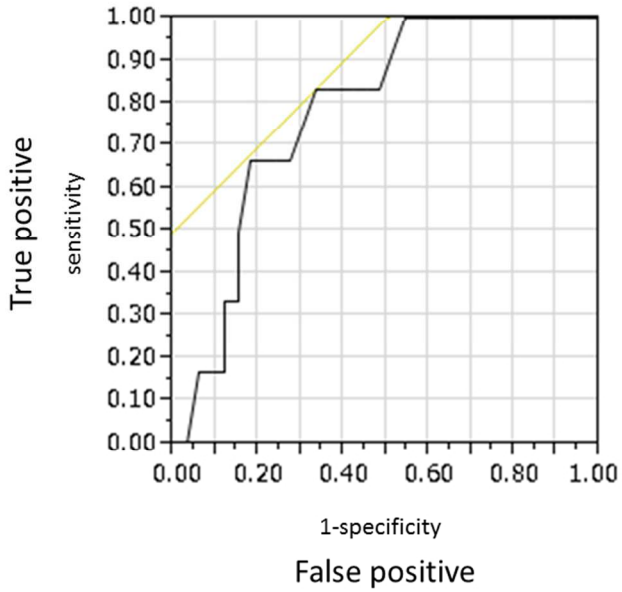

Supplemental figure 5

Supplemental Figure 5
Receiver operating characteristic (ROC) curve for prediction of G3 with tumor size. The cut-off value of tumor size between the G1, G2, and G3 determined by the ROC analysis was 30mm.

254x190mm (96 x 96 DPI)